Available online at www.sciencedirect.com
SCIENCE DIRECT
Catalysis Today 107–108 (2005) 338–345
CATALYSIS TODAY
www.elsevier.com/locate/cattod

Cu, Mn and Co molybdates derived from novel precursors catalyze the oxidative dehydrogenation of propane

Luz Amparo Palacio [a,b,*], Adriana Echavarría [c], Ligia Sierra [c], Eduardo A. Lombardo [d]

[a] *Departamento de Ingeniería Química, Universidad de Antioquia, AA 1226 Medellín, Colombia*
[b] *Laboratorio de Catalizadores y Adsorbentes, Universidad de Antioquia, Medellín, Colombia*
[c] *Instituto de Química, Universidad de Antioquia, AA 1226 Medellín, Colombia*
[d] *INCAPE (FIQ, UNL-CONICET), Santa Fe, Argentina*

Available online 10 August 2005

Abstract

The activity of various transition metal molybdates in the oxidative dehydrogenation of propane was tested. A series of nine molybdates of Zn, Cu, Co, Fe and Mn were synthesized by either a hydrothermal or a precursor method. The catalysts were characterized by X-ray diffraction (XRD), atomic absorption (AA), laser Raman spectroscopy (LRS), and scanning electron microscopy (SEM). The reaction was carried out at atmospheric pressure in a temperature range of 400–600 °C. The copper, cobalt and manganese molybdates were the best performing catalysts. The latter one reached selectivities around 50% at 20% conversion. All the catalysts kept the original structure after reaction. The best and most stable formulation was a cobalt molybdate, the only solid that maintained its surface area after reaction.

Keywords: Oxidative dehydrogenation; Metallic molybdates; Propane; Propene; Synthesis

1. Introduction

The oxidative dehydrogenation of C_2–C_5 paraffins is an intensively explored pathway to produce olefins. The driving force behind this search is the increased demand of short chain alkenes expected in the years to come since they are essential building blocks for high-quality gasoline, diesel fuel, and a variety of chemicals and polymers. The main source of C_2–C_4 paraffins is of course natural gas [1].

Focusing on propane oxydehydrogenation, the catalysts with the highest yields (ca. 20%) reported so far are the zinc and magnesium vanadates [2] and formulations of K/Mo supported over silica and titania mixed oxides [3]. Several catalysts containing molybdenum and a variety of transition metals have been tested. Some of them are molybdenum oxides supported on Nb_2O_5, TiO_2, Al_2O_3, SiO_2, MgO and ZrO_2 [4,5]. However, the majority of molybdenum catalysts studied so far are unsupported, usually molybdates of varying structures containing nickel, manganese, magnesium or cobalt [6–9]. The best results reported up till now are those of Mazzocchia et al. [10] using nickel molybdate $NiMo_{1.5}O_{5.5}$. They obtained the maximum propane conversion (29%) at 600 °C with selectivity to propene of 62.5%.

In a previous work, Ion et al. [11] assayed different metal molybdates in the temperature range of 350–500 °C and found that cobalt molybdate was a good catalyst. The catalytic behavior was markedly affected by the solid composition. Although they gave the chemical formula of each catalyst, they did not include any structural information, e.g. in the case of $CoMoO_4$, several different crystalline forms are known to exist and they could possibly exhibit different catalytic behavior.

This work is concerned with the use of nine molybdates (Cu, Mn, Co, Fe and Zn) synthesized and characterized in our laboratory in the oxidative dehydrogenation of propane. The aging of the best performing catalysts was investigated and connected to the evolution of their textural and structural characteristics with time on stream.

* Corresponding author.
E-mail address: lpalacio@udea.edu.co (L.A. Palacio).

0920-5861/$ – see front matter © 2005 Elsevier B.V. All rights reserved.
doi:10.1016/j.cattod.2005.07.031

Table 1
Synthesis conditions of the precursors

Catalyst	Preparation method[a]	Gel molar composition	T (°C)	t (h)
CoMoϕx	Hydrothermal	$H_2N(CH_2)_2NH_2$:Na_2MoO_4:$Co(NO_3)_2$:175H_2O	200	48
CoMo11	Precursor	Na_2MoO_4:$CoCl_2$:170.7H_2O	–	–
CuMoϕy	Hydrothermal	MoO_3:0.5$CuSO_4$:NH_4OH:175H_2O	170	24
CuMo21	Precursor	Na_2MoO_4:$CuCl_2$:135H_2O	–	–
FeMoϕx	Hydrothermal	2Na_2MoO_4:0.5Na_2O:$FeCl_2$:173H_2O	150	24
FeMo20	Precursor	Na_2MoO_4:$FeSO_4$:176H_2O	–	–
MnMo10	Hydrothermal	MoO_3:$MnCl_2$:2NH_4OH:184H_2O	25	21
ZnMo72	Hydrothermal	MoO_3:$ZnCl_2$:2NH_4OH:180H_2O	25	2
ZnMo75	Precursor	Na_2MoO_4:$ZnCl_2$:170H_2O	–	–

[a] See text for method description.

2. Experimental

2.1. Catalysts preparation

Two zinc, two copper, two cobalt, two iron molybdates and one manganese molybdate were synthesized. Five of them synthesized by a hydrothermal method followed by calcination at 600 °C for 3 h. The remaining four were prepared by the precursor method. In the hydrothermal method, two previously prepared solutions were mixed together and stirred for 2 h. When needed, a template was added. Such was the case of CoMoϕx, whose synthesis requires the addition of ethylendiamine in order to obtain the ϕx phase [12]. The gel obtained was kept at the temperature indicated in Table 1 for the period also shown there. The molybdenum solutions were prepared from either sodium molybdate or MoO_3 and ammonium hydroxide. The second solution was prepared by dissolving the transition metal salt in water.

In the precursor method, solutions of sodium molybdate and the desired transition metal were mixed in adequate proportions to form a homogeneous gel at room temperature. After filtration, the solid obtained was dried at 120 °C and heated at 2 °C/min in air up to 600 °C and kept at this temperature for 3 h. Further information about the preparations is provided in Table 1. Note that the solids labeled CoMoϕx, CuMoϕy, FeMoϕx and MnMo10 before calcination are new materials obtained in our laboratory [12–14].

The synthesis conditions of the precursors shown in Table 1 are the result of previous studies during which they were optimized in order to get pure and crystalline materials. In some cases, new crystalline phases never synthesized before they were obtained. Moreover, subtle modifications to the procedures may lead to the appearance of different phases.

2.2. Catalysts characterization

2.2.1. Analysis of the elements

The concentration of Mo, Na, Co, Cu, Fe, Mn and Zn was determined by atomic absorption (AA) in a Unicam Solar equipment.

2.2.2. Surface area

Micromeritics ASAP 2010 was used in order to determine the surface area of the catalysts before and after reaction.

2.2.3. X-ray diffraction (XRD) data

The diffractograms were obtained using a Rigaku Miniflex (radiation Cu Kα $\lambda = 1.5418$ Å) powder diffractometer, operated at 40 kV and 30 mA. The samples were run in a range of 3–40° (2θ) at a rate of 2°/min. The phases were identified using the powder diffraction file (PDF) and the inorganic crystal structure databank (ICSD).

2.2.4. Raman spectroscopy data

The Raman spectra were recorded with a Jasco laser Raman spectrometer model TRS-600-SZ-P, equipped with a charge coupled device (CCD) with the detector cooled to about 153 K using liquid N_2. The excitation source was the

Table 2
Identification of the phases present in the catalysts

Catalyst	Crystalline phase	PDF[a]	ICSD[a]	Amorphous phase[b]	%Na[c]	%Mo[c]	%M[c]
ZnMo75	$Na_2Zn_5(MoO_4)_6$	84–0365	201162	$ZnMo_2O_7$	5.2	39.8	30.4
ZnMo72	$ZnMoO_4$	72–1486	17030		–	38.9	28.9
MnMo10	$MnMoO_4$	27–1280	15615	–	–	43.5	24.6
CuMoϕy	$CuMoO_4$	73–488	411384	–	–	45.1	26.8
CuMo21	$Cu_3Mo_2O_9$	24–55	9155	–	–	32.8	31.9
FeMo20	$Fe_2(MoO_4)_3$	83–1701	100606	–	–	43.0	24.9
FeMoϕx	$NaFe(MoO_4)_2 + (1/2)Fe_2O_3$	30–1195	–	–	6.8	42.4	20.8
CoMo11	$CoMoO_4$	25–1434	23808	–	–	42.9	27.7
CoMoϕx	$CoMoO_4$	21–868	15615	Na_2O	5.2	45.2	29.8

[a] PDF: powder diffraction file, ICSD: inorganic crystal structure databank.
[b] They come out from the mass balance, taking into account the chemical analysis and the crystalline phases identified by XRD.
[c] Analytical data obtained by atomic absorption.

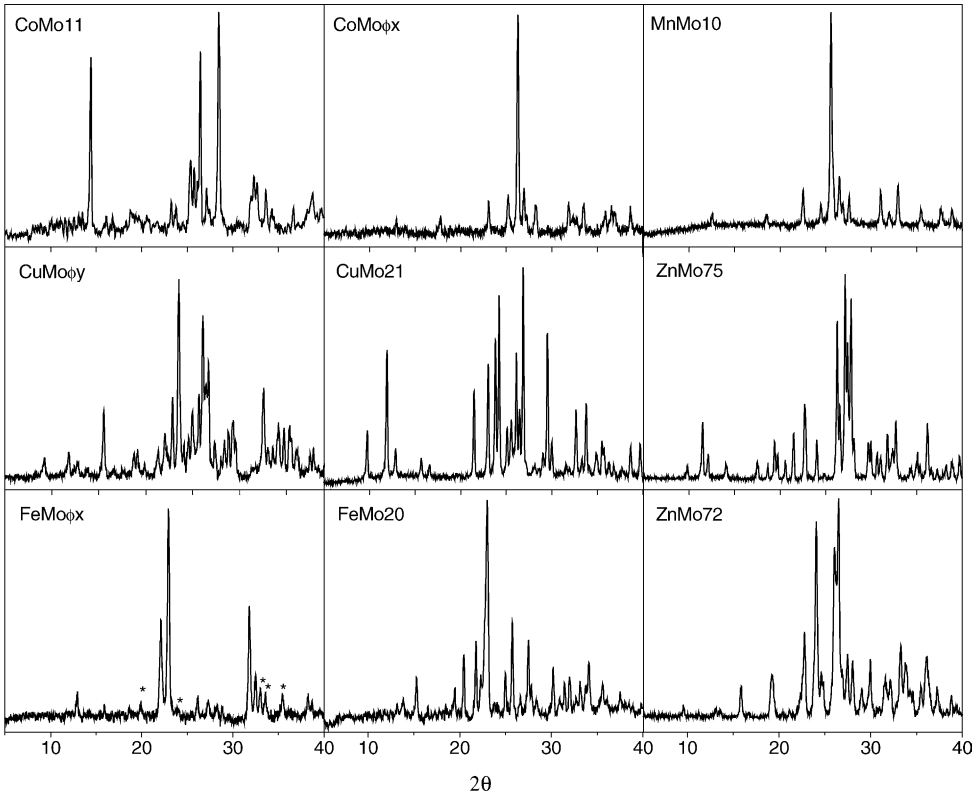

Fig. 1. Diffractograms of the fresh catalysts. No differences were observed after use. Radiation Cu Kα λ = 1.5418 Å, operated at 40 kV and 30 mA, range of 3–40° (2θ) at 2°/min.

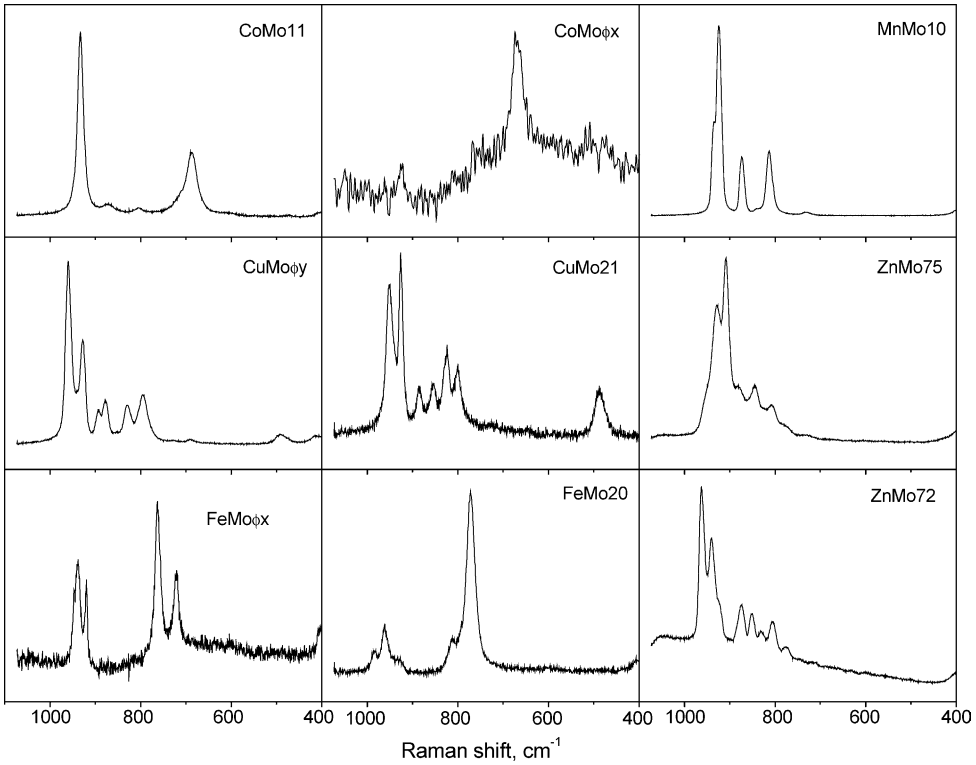

Fig. 2. Raman spectra of the fresh catalysts. The used ones exhibited the same profiles. Excitation source was the 514.5 nm, laser power at 40 mW.

Table 3
Yield to olefins at 600 °C

	Catalyst								
	ZnMo75	ZnMo72a	MnMo10	CuMoϕy	CuMo21	FeMo20	FeMoϕx	CoMo11	CoMoϕx
Propene	2.6	2.4	10.1	4.7	1.6	4.4	1.3	1.8	5.8
Ethene	0.8	0.6	3.6	1.0	0.5	1.1	0.3	1.1	0.9
Surface area (m^2/g)									
Fresh	1.4	6.6	4.0	5.6	3.7	2.0	0.9	5.3	6.2
Used	0.3	4.3	1.1	0.1	0.1	0.1	0.3	1.2	6.3

Space velocity 6000 ml/(g h) (29% C_3H_8, 71% air).

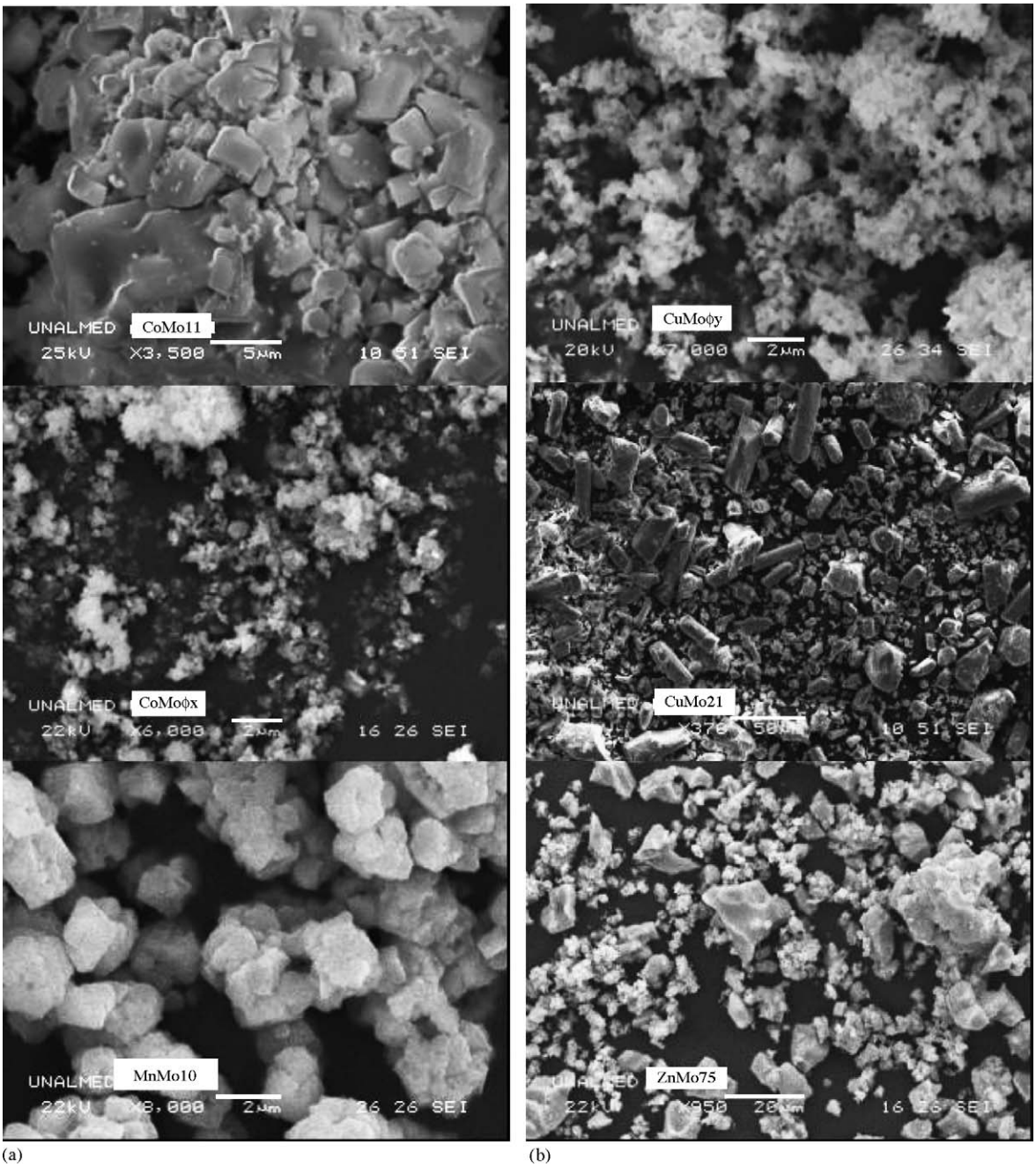

(a) (b)

Fig. 3. Micrographs of the fresh catalysts.

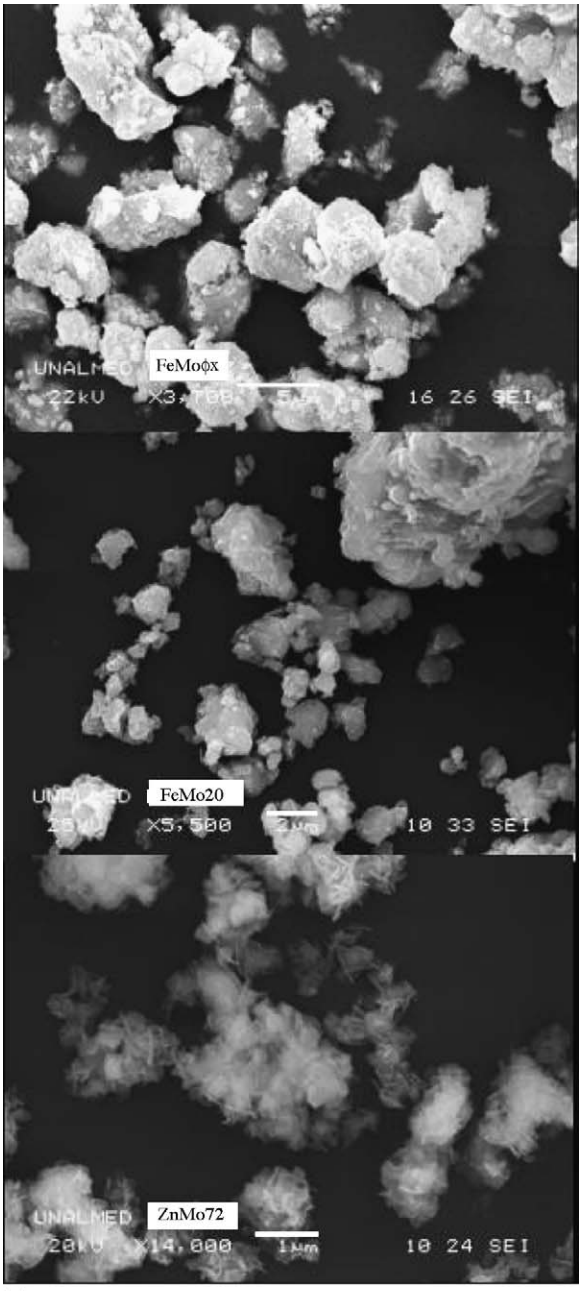

(c)

Fig. 3. (*Continued*).

514.5 nm line of a Spectra 9000 Photometrics Ar ion laser. The laser power was set at 40 mW. All the spectra were recorded with the samples under ambient conditions. The powdered solid was pressed as a thin wafer about 1 mm thick.

2.2.5. Scanning electron microscopy (SEM)

The catalysts morphology was observed using a JEOL JSM-59 LV microscope.

2.3. Catalytic tests

A fixed-bed reactor containing 1.0 g of catalyst was used to perform the catalytic tests. All products were analyzed on line using a Shimadzu 9 A chromatograph equipped with two columns, a Molecular 5A and a PorapakQ one. The reaction was carried out at atmospheric pressure in the temperature range of 400–600 °C. The gases used were propane 98% and dry air supplied by AGAfano. The reactant mixture contained 29% propane and 71% air. This corresponds to a propane/oxygen molar ratio of 2 (stoichiometric ratio). The feed composition was chosen to be above the flammability limit under reaction conditions. Another reason for selecting this feed composition is to use air instead of oxygen, a cheaper choice for practical applications. Blank tests were performed with the empty reactor at 600 °C. No propene formation was detected in this way.

3. Results and discussion

3.1. Chemical composition and structure

3.1.1. X-ray data

The diffractograms of the synthesized solids are shown in Fig. 1. The phases identified in this way are given in Table 2. It can be seen that all the catalysts are made up of either binary or ternary mixed oxides, the majority of them single phase. The CoMoϕx and MnMo10 catalysts are isomorphic. Note that the two cobalt molybdate phases have the same chemical formula but different structures. The FeMoϕx catalyst is a mixture of two crystalline compounds; the reflections of the Fe_2O_3 phase are indicated with asterisks in the diffractogram.

The chemical composition of all the solids is reported in the last three columns of Table 2. In most cases, the chemical formula calculated from the chemical analysis coincided with the one corresponding to the crystalline phase detected by XRD. When this was not the case, the mass balance allowed the detection of amorphous phases, as seen in the first and last rows of Table 2.

3.1.2. Laser Raman data

Fig. 2 shows the Raman spectra of the catalysts. Different regions of each wafer were explored in every sample. The beam diameter is ca. 1–10 μm. The three or four spectra obtained with each wafer were identical, indicating that the solids are homogeneous.

The molybdenum–oxygen stretching frequency in the Raman spectra for each catalyst was calculated using the bond distances corresponding to each structure and the correlation of Hardcastle and Wachs [15]. From crystallographic data it is concluded that they are made up of different tetrahedrons accommodated in the crystalline structure with the exception of CoMo11, which has one additional molybdenum atom with coordination 3. For this reason the Raman shifts are different despite the fact that all catalysts have molybdate groups in their composition.

It was verified that each band appearing in the spectra of Fig. 2 corresponded to Mo–O stretching frequencies of the

polyhedrons of the catalysts. There is only one spectrum whose Raman signals do not adjust to the calculated one, FeMo20, whose structure is made up of six molybdenum tetrahedrons, all with very similar bond distances (between 1.740 and 1.774 cm^{-1}). This would give origin to two bands at 824 and 785 cm^{-1}. However, there are three additional bands at 990, 967 and 934 cm^{-1}. This is difficult to explain because according to the chemical analysis and the XRD data there are no impurities in this material.

The manganese molybdate has two types of molybdenum tetrahedrons. The first tetrahedron is formed by a Mo1 bonded to four oxygen atoms with different bond distances: for two O3 oxygen atoms the distance is 1.731 Å and for two O4 oxygen atoms the distance is 1.796. Therefore, the Mo1–O3 and Mo1–O4 stretching vibrations in the spectrum correspond to shifts of 875 and 814 cm^{-1}, respectively. In the same way, the second tetrahedron formed by Mo2 is bonded to two O5, one O2 and one O1 atoms, whose bond distances are 1.724, 1.737 and 1.852 Å, respectively. This would correspond to Raman shifts of 925, 875 and 733 cm^{-1}.

Another example concerns the cobalt molybdates which in spite of having the same composition possess different structures. This is clearly seen in the corresponding diffractograms of Fig. 1 and the Raman spectra of Fig. 2. CoMo11 is formed by a Mo1 molybdenum coordinated to two O3 oxygen atoms and a O4; and by a tetrahedral Mo2 bonded to two O2 oxygen atoms and two O1. The corresponding Raman shifts are 936, 691 and 600 cm^{-1}. On the other hand, CoMoϕx is made up of two molybdenum tetrahedrons. In the first one, Mo is bonded to two pairs of equal oxygens while the second Mo is connected to another pair of different oxygens. This formation generates bands in the Raman spectrum with shifts of 925, 804 and 673 cm^{-1}.

The structural features obtained from the Raman spectra are fully consistent with the information retrieved from the X-ray diffractograms. Note that neither the Raman fingerprints nor the X-ray profiles changed after the catalytic runs. That was not the case with the surface area (vide infra).

3.1.3. Surface area

Table 3 shows the BET areas of both the fresh and the used catalysts. Only CoMoϕx maintains its surface area after use while all the others, except ZnMo72a, show drastic decreases after being on stream at 600 °C for a few hours. Values below ca. 1 m^2/g are only reported as an indication of the sharp decrease in surface area of the corresponding solids.

3.1.4. SEM

Fig. 3 shows the micrographs of the nine fresh catalysts. They have different morphologies and they all exhibit a very homogeneous appearance except for iron molybdate FeMoϕx in which the crystalline molybdate is covered with small spherulites which could correspond to the hematite phase (Fe_2O_3). The particle sizes corresponding to each compound are as follows: CoMoϕx, ZnMo72 and FeMo20, less than 1 μm; CoMoϕx and MnMo10, around 2 μm; CoMo11 and FeMoϕx, around 5 μm; ZnMo75, around 10 μm; and CuMo21 around 20 μm.

3.2. Catalytic activity and stability

The majority products detected during the oxidative dehydrogenation of propane were propene, CO, CO_2, ethene and methane. The propane conversion and selectivity to propene for each catalyst are shown in Fig. 4. Each point is the average of three successive analyses of the product

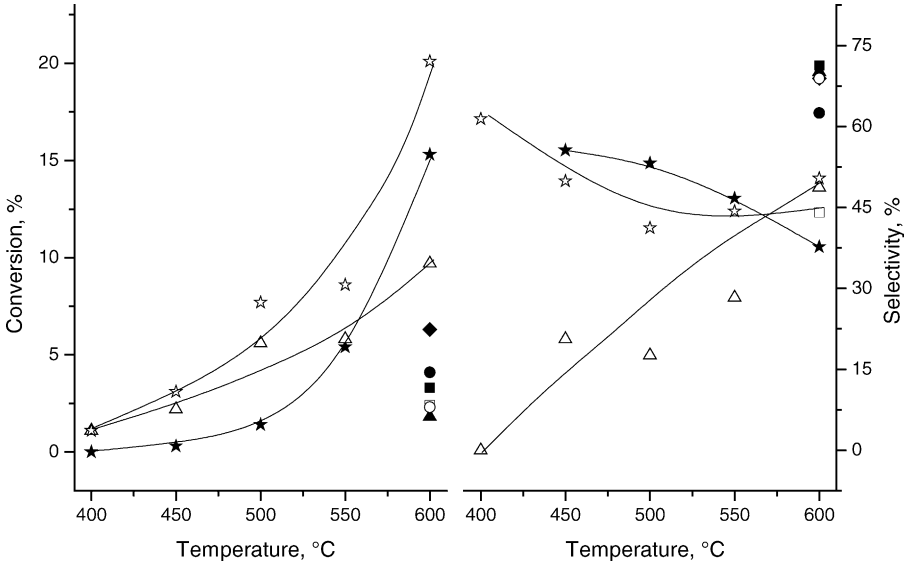

Fig. 4. Catalytic behavior of metal molybdates. Space velocity 6000 ml/(g h) (29% C_3H_8, 71% air): (■) ZnMo72; (●) ZnMo75; (▲) FeMoϕx; (◆) FeMo20; (★) CoMoϕx; (□) CoMo11; (○) CuMo21; (△) CuMoϕy; (☆) MnMo10.

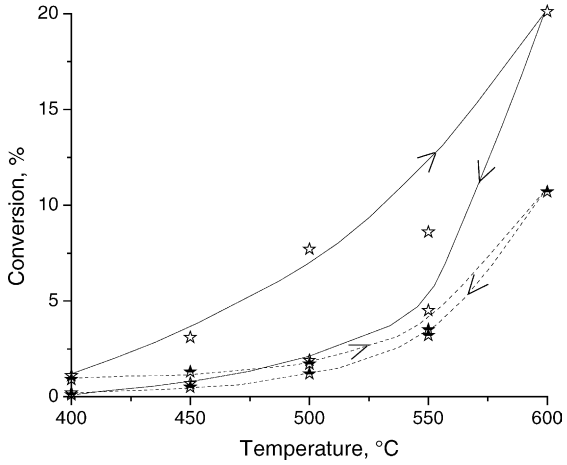

Fig. 5. Stability of the MnMo10 catalyst. Reactant composition 29% C_3H_8, 71% air, space velocity 6000 ml/(g h), C_3H_8/O_2 ratio = 1: (☆) first cycle; (★) second cycle. The direction of the arrows indicate whether the temperature was increased or decreased during a sequence of measurements.

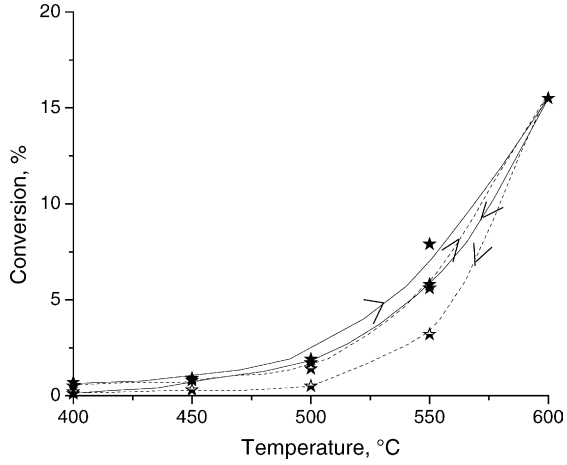

Fig. 7. Stability of the CoMoϕx catalyst. Reactant stream composition 29% C_3H_8, 71% air, space velocity 6000 ml/(g h), C_3H_8/O_2 ratio = 2: (★) first cycle; (★) second cycle.

stream. Note that the MnMo10, CuMoϕy and CoMoϕx catalysts are the only active ones in the whole temperature range. The others are active solely at 600 °C. This is why Fig. 4 exclusively shows data at 600 °C for ZnMo75, ZnMo72, FeMoϕx, FeMo20, CuMo21 and CoMo11. It is concluded that the most active catalyst is MnMo10 and the most selective ones at similar conversion levels are CoMoϕx and MnMo10.

Table 3 shows that the best yields at 600 °C were obtained with MnMo10, CuMoϕy and CoMoϕx. Figs. 5 and 6 show, however, that the former two solids sharply deactivate when the conversion is measured by decreasing the reaction temperature after reaching 600 °C in the ascending leg. Much more stable was CoMoϕx (Fig. 7). To investigate the cause of this behavior, the diffractograms and the Raman spectra of the used catalysts were recorded. In all cases the used solids exhibited the same fingerprints as the fresh ones. Thus, the only difference observed among these three solids is that the most stable catalyst, CoMoϕx, is the only one that retains the same surface area after use. The sharp decrease in surface area of all the other formulations could be a consequence of the disappearance of the internal pores due to the sinterization of the solids since no change in crystal structure was detected.

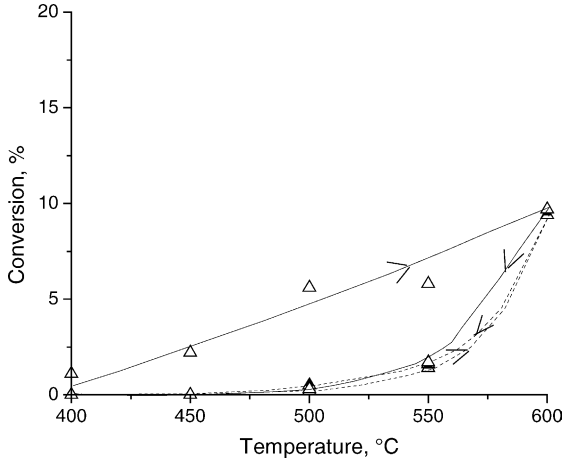

Fig. 6. Stability of the CuMoϕy catalyst. Reactant stream composition 29% C_3H_8, 71% air, space velocity 6000 ml/(g h), C_3H_8/O_2 ratio = 2: (△) first cycle; (▲) second cycle.

4. Conclusions

This study was conducted to evaluate the catalytic performance and the stability of nine molybdates that we synthesized. All the catalysts were shown to be structurally stable under the reaction conditions used in this study. Most of them, however, showed a sharp decrease in surface area after being on stream at 600 °C for several hours. Mn, Cu and Co yielded the most active catalysts. Note, however, that the type of structure also plays an important role in catalytic performance (Table 3). By far the most stable one was CoMoϕx, the only solid that maintained the surface area after being on stream at 600 °C. The reason behind this high textural stability is a matter of further research.

Acknowledgements

This work was carried out with the financial support received from COLCIENCIAS. Thanks are given to Elsa Grimaldi for the English language editing.

References

[1] M. Baerns, O. Buyevskaya, Catal. Today 45 (1998) 13.
[2] H. Kung, M. Chaar, U.S. Patent 4 777 319 (1988).
[3] U. Ozkan, R. Watson, U.S. Patent 6 521 808 (2003).
[4] F. Meunier, A. Yasmeen, J. Ross, Catal. Today 37 (1997) 33.

[5] K. Chen, S. Xie, E. Iglesia, A. Bell, J. Catal. 189 (2000) 421.
[6] A. Kaddouria, C. Mazzocchia, E. Tempesti, Appl. Catal. A 169 (1998) L3.
[7] L. Cadus, O. Ferreti, Appl. Catal. A 233 (2002) 239.
[8] Y. Yoon, K. Suzuki, T. Hayakawa, S. Hamakawa, T. Shishido, K. Takehira, Catal. Lett. 59 (1999) 165.
[9] M. Barsan, F. Thyrion, Catal. Today 81 (2003) 159.
[10] C. Mazzocchia, E. Tempesti, C. Aboumrad, U.S. Patent 5 086 032 (1992).
[11] Y. Ion, N. Fujikawa, W. Ueda, Y. Moro-oka, K. Lee, Catal. Today 24 (1995) 327.
[12] L. Palacio, A. Echavarría, C. Saldarriaga, Intern. J. Inorg. Mater. 3 (2001) 367.
[13] L. Palacio, A. Echavarría, C. Saldarriaga, Stud. Surf. Sci. Catal. 135 (2001) 2888.
[14] L. Palacio, Ph.D. thesis, School of Chemical Engineering, Universidad Nacional del Litoral, Santa Fe, Argentina, 2001.
[15] F. Hardcastle, I. Wachs, J. Raman Spectrosc. 21 (1990) 683.